REGISTRATION USING PROBABILISTIC PLANAR MATCHING WITH APPLICATION IN INDOOR MAPPING

Arpan Kusari
Research Scientist
Ford Motor Company
Dearborn MI 48124
arpan.kusari@gmail.com

ABSTRACT

With the use of laser scanning technology in structured environments on the rise, there has been a lot of work done in matching 3D laser scans to a common coordinate frame using planar surfaces. However, these methods depend on heuristic based planar matching algorithms which lack robustness to noise and outliers. I present a probabilistic planar matching technique to perform pairwise registration based on the principle of maximum entropy. The planar correspondences are treated as a latent variable leading to a maximum likelihood estimation in the expectation-maximization framework. Simulated transformation parameters are used to estimate the weights of the cost function. 10 pair of LiDAR scans are collected in the indoor environment with artificial targets and actual transformation parameters are calculated using manual registration. These pairs are then registered using the proposed method and Generalized-ICP (GICP) (Segal et al, 2009) which are then compared and contrasted.

KEYWORDS: registration, maximum entropy, expectation-maximization

INTRODUCTION

Mobile mapping technologies combine the benefits of absolute and relative positioning devices and imaging sensors to locate features in a global framework (Li, 1997). Indoor mapping utilizes similar sensors to map interior of the buildings
without the availability of the absolute positioning such as Global Navigation Satellite System (GNSS) (El-Hakim et al, 1997). Indoor mapping is used frequently to model and analyze interior architectures using 3D LiDAR scanners. Utilizing multiple scans from different sensor positions can lead to a very dense and accurate model that can be utilized in variety of applications such as emergency response and 10 augmented reality. However, the scans need to be registered to a common frame of reference to form a cohesive model. The usual choice is to use artificial markers and constrain the scans using the markers. However, placing markers at strategic points so that none of the scans are under-constrained, can be very time-consuming and labor intensive (e.g. Riegl scan software RiScan).

A popular alternative is to use Iterative Closest Point algorithm (Besl and Mckay, 1992) which uses an iterative estimation model to find the transformation by minimizing sum of squared distances between corresponding points for each pair of scans (Khoshelham, 2010). It suffers from two particular drawbacks: initial estimates close to global minima are required to prevent the problem being stuck in local minimum and there is no guarantee of convergence. A lot of research has been done to make ICP robust and remove the drawbacks by assigning differential weights to the LiDAR point pairs. A variety of factors have been used to weigh the point pairs such as distance, color, curvature etc. (Douadi et al, 2006, Schutz et al, 1998, Rusinkiewicz and Levoy, 2001). Rangarajan et al introduced a probabilistic matching of point sets based on gaussian weight (soft-assign (Rangarajan et al, 1997)) and mutual information (Rangarajan et al, 1999), but the scans needed to have comparable sets of points. EM-ICP proposed by (Granger et al, 2001) provides a probabilistic matching of closest points within the expectation maximization framework leading to a more robust solution while still being dependent on gaussian weight. Another probabilistic matching technique, Generalized ICP (GICP), was proposed by (Segal et al, 2009) which uses the local planar structure of both scans to register the point clouds together. This method was shown to outperform both standard ICP and point-to-plane ICP and has been used in the industry as a stable option to provide registration between point datasets.

A different formulation for registration of point datasets is the feature-based registration approach (Higuchi et al, 1995, Chua and Jarvis, 1996, Rabbani et al, 2007, Brenner et al, 2008). In this method, several salient primitive features are extracted from the datasets and used to register the scans. A method based on extraction of planes was proposed by (He et al, 2005). The method required complete plane patches and did not work on occluded planes. (Wang and Tseng,

2004) used an octree implementation to divide the dataset and then search for best fit planes. (Bae and Lichti, 2004) used geometric primitives and neighborhood search to register partially overlapping point clouds. (Gruen and Acka, 2005) proposed a method that estimated the transformation from corresponding 3D surface patches. (Dold and Brenner, 2006) used extracted planar patches from the 3D terrestrial scanning data and also gave a quantitative criterion to formulate the angles between the normal vectors of the planes to use as constraints for _finding the corresponding planes in the point clouds. (Pathak et al, 2010) used Minimally uncertain Maximal Consensus (MUMC) method by minimizing uncertainty volume to find planar correspondences and showed that robust transformation parameters can be calculated using planar patches.

The methods referenced above used some form of constraints to prune out the search space and maximize the correspondences. These however, suffer from being computationally intensive and time expenditure from hand tuning of the pruning parameters. In this paper, we propose a robust probabilistic planar matching approach to register point clouds. The use of latent variable formulation is somewhat similar to the EM-ICP with the use of principle of maximum entropy to denote the probability (although not explicitly stated). However, since we use planes in place of points, a different cost function is to be formulated and the calculation of the transformation parameters becomes more complex. The resulting derivation leads to adaptation of rotation and translation equations given by (Brenner et al, 2008).

The paper is structured as follows: in Section 2, the derivation of the method is provided; Section 3 gives the results of the coarse orientation using simulations for different rotations and translations and comparing them to GICP and Section 4 provides the conclusions of the work.

METHODOLOGY

Let S_1 and S_2 be the scans at 1st and 2nd time instance respectively. The first part of the problem is extracting the planar features in each scan using a fast, reliable procedure. The planar features p_1 and p_2 need to be matched and the transformation parameters calculated. The matching is performed based on the principle of maximum entropy with a cost function which is designed to be discriminative both in the normal and distance of plane to origin. The matching is then used to update the transformation parameters.

Planar feature extraction

LiDAR points are samples from the surface of the objects that are scanned. Usually the scans are stored incrementally in time without any consideration to coherence properties (Wang and Tseng, 2011). Inspecting the coherence properties of the local neighborhood is an important consideration in extraction of high-level features from the points. There are many different strategies for planar feature extraction, using top down (e.g., split and merge), bottom-up (e.g., region growing) or global (e.g., Hough transform) approaches. In this work, a bottom-up approach using uniform voxel is employed. The uniform voxel approach divides the entire 3D space into equal cubical spaces. A parallelized version of the robust estimation of multiple inlier structures algorithm proposed by (Yang and Meer, 2016) is used to extract the planes within each voxel. The neighboring information is required for the region-growing process. For each voxel, 27 neighboring nodes are easily computed using the index of the given voxel. The region-growing algorithm finds the contiguous planar regions based on coplanarity and distance from the plane.

There are two ways to compare planes to find the similar planes:

- Hard thresholding - User specified threshold values are given for coplanarity measure (n_{thres}) and distance from plane (d_{thres}). The comparison equations are given as:

$$n_{1,i}.n_{2,j} > \alpha_{thres} \quad (1)$$

$$n_{1,i}.c_{2,j} < d_{thres} \quad (2)$$

  where $n_{1,i}$ and $n_{2,j}$ are the planar normals for i^th plane in p_1 and j^th plane in p_2 and $c_{2,j}$ is the planar centroid of j^th plane in p_2.

- Soft thresholding - When two planar patches of a single planar surface are combined, the resulting planar patch should be similar to the initial planar patches. This observation is used to come up with a soft thresholding paradigm given by:

$$|\, n_{res}.n_{1,i}| \cong |n_{res}.n_{2,j}| \quad (3)$$

$$| \ n_{res}.c_{1,i}| \ \cong |n_{res}.c_{2,j}| \tag{4}$$

where n_{res} is the normal vector of the resulting planar patch.

The hard thresholding method is faster while the soft thresholding method has to compute the resulting planar patch at each step. But the soft thresholding is more adaptive and does not involve any user supplied threshold. Thus, we use the soft thresholding method in this work.

E-step - Uncertain matches based on cost function

In the expectation step, we calculate the optimal correspondences based on a given transformation. Due to movement of the sensors in between two scans S_1 and S_2 and due to noise and occlusions, it is almost never possible to find exact matches between planes. We define a matrix A where Aij gives the weight of matching between $p_{1,i}$ and $p_{2,j}$. We define the matches between the planes using the principle of maximum entropy (Jaynes, 1957). According to the principle, the distribution over planar matches can be constrained to match the expectations under a given cost function while being no more committed to any particular distribution than the constraint requires. Thus, matches with equal cost have equal probabilities and matches with lower cost are exponentially more preferred (Equation 5).

$$A_{ij} = P\left(match\middle|C_{ij}\right) = \frac{1}{Z}e^{-C_{ij}} \tag{5}$$

where C_{ij} is the cost function for $p_{1,i}$ and $p_{2,j}$ and Z is the partition function or the normalization function. Using this principle automatically provides a robust matching criterion for defining matches between partially occluded scans while moving away from hand-tuned parameters.

The cost function has to be designed to be discriminative enough to penalize dissimilarity between planes. There are two different conditions of calculating similarity: angle between the planar normals and difference in distances to the origin. For the first part, the goal is to penalize absolute value of the dot product with values farther from 1. The goal in the second part is to penalize normalized difference in distances. Keeping these in mind, the cost function is constructed as below:

$$C_{ij} = w_n|\theta|^2 + w_d\left|d_{1,i} - d_{2,j}\right|^2 \tag{6}$$

where θ is the angular distance ($0 \leq \theta \leq \pi$), $d_{1,i}$ and $d_{2,j}$ are the planar distances ($d_{1,i}, d_{2,j} \in [0, d_{max}]$) and, w_n and w_d are the weights given to the two parts respectively.

M-step - optimal transformation parameters

Since the optimal matching matrix has been calculated, we can optimize the criterion w.r.t. the transformation. In case of perfect correspondences, the optimal rotation matrix can be defined as minimization of the quadratic error of $\sum_i \left|\left|R.n_{2,i} - n_{1,i}\right|\right|^2$ or equivalently maximization over the sum of the dot products (Brenner et al, 2008). Following the derivation proposed by (Horn, 1987), using unit quaternions, a rotation **Rn** can be represented as $\boldsymbol{q}\dot{\boldsymbol{n}}\boldsymbol{q}*$, where $\boldsymbol{q}$ is the unit quaternion, $\dot{\boldsymbol{n}}$ is the quaternion representation of normal vector n and $\boldsymbol{q}*$ is the conjugate of $\boldsymbol{q}$.

Maximizing the sum of the dot products, a matrix N is constructed such that

$$N = \sum_i N_{2,i}^T N_{1,i} \tag{7}$$

where N is the matrix representation of $\dot{n}$. This can be seen as a specialized case when perfect planar matches are defined, with

$$A_{ij} = \begin{cases} 1, & if\ i = j \\ 0, & otherwise \end{cases} \tag{8}$$

Thus for uncertain matches, the Equation 7 can be augmented as:

$$N = \sum_{i} \sum_{j} A_{ij}\, N_{2,i}^{T} N_{1,i} \tag{9}$$

The quaternions can be given by the eigenvector of N corresponding to the largest eigenvalue and the rotation matrix can be obtained as a Rodriguez matrix.

The calculation of the translation is trickier in case of uncertain matches. For binary correspondences, the translation is found after the rotation using an ordinary least squares (OLS) criterion

$$t = (M^T M)^{-1} M^T l \tag{10}$$

where

$$M = \begin{bmatrix} n_{1,i}^{T} \\ n_{1,j}^{T} \\ n_{1,k}^{T} \\ \vdots \end{bmatrix}$$

and

$$l = \begin{bmatrix} d_{1,i} - d_{2,i} \\ d_{1,j} - d_{2,j} \\ d_{1,k} - d_{2,k} \\ \vdots \end{bmatrix}$$

However, OLS is not robust to wrong matches and outliers. So, instead, an approximate least trimmed sum of squares (LTS) criterion is used (Shen et al, 2013). LTS does not have a closed form solution similar to OLS and is concave. Instead, starting with a complete M and l, a convex optimization is run to remove outliers by minimizing weights and removing weights very close to 1. The optimization problem is defined by:

$$\begin{aligned} \underset{m,w,k}{\text{minimize}} \quad & 1^T k - \sum_i l_i^2 w_i \\ \text{subject to} \quad & \left\| \begin{bmatrix} 2m_i \\ w_i - k_i \end{bmatrix} \right\| \le w_i + k_i \\ & \mathbf{M^T} m = \mathbf{M^T W} d \\ & 1^T w = p \\ & 0 \le w \le 1 \end{aligned} \tag{11}$$

where w_i is the weight of each observation, W is the diagonal weight matrix and p is the number of outliers intended to be removed at every iteration. The reader is referred to (Shen et al, 2013) for detailed description of the optimization process.

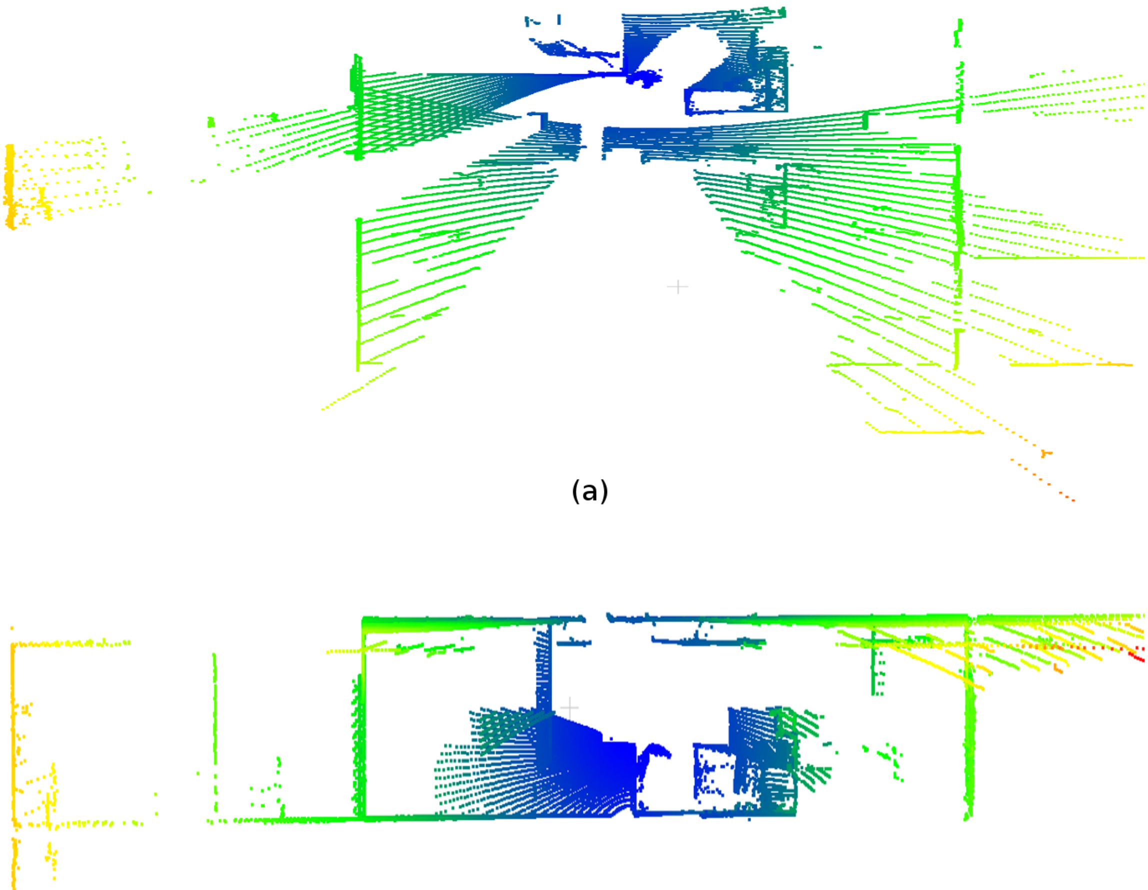

(a)

(b)

Figure 1. Lidar scans of the environment (a) Top view (b) Side view

RESULTS

Finding optimal weights

In order to compute the coarse registrations of best fit planes from point clouds, the optimal weights, wn and wd of the cost function have to be determined. In this work, I used a laser scan as a model and transformed laser scans (using simulated translations and rotations) as scene datasets. The laser scan used is from an indoor environment using a Velodyne HDL-32E scanner (Figure 1) with primarily vertical and horizontal planes with point accuracy of 0.02 m (at 25 m) (Velodyne Manual). Simulations of rotations and translations {0, 0.1,…, 1}º range and {0, 0.05,…, 0.5}m range are used in all three axes. Weights are increased by a factor of $10 \in \{1, 10^6\}$ for both w_n and w_d. Use of simulated transformation parameters with the actual scan is helpful in capturing a wide swath of transformations with known ground truth while having a representative measurement noise. Performance is then analyzed by convergence to the correct solution.

Three representative simulated transformations are shown in Figure 2 with the x and y-axes being $\log_{10} w_n$ and $\log_{10} w_d$. The left side plots have the z-axis as the sum of difference of the actual rotation angles and estimated rotation angles in degrees. The right side plots have the z-axis as the sum of difference of the actual translations and estimated translations in meters. In the first pair of plots, a rotation of 0.1º is applied to all three axes. In the second pair of plots, a translation of 0.5 m is applied to all three axes. In the third pair, a rotation of 0.1º and a translation of 0.1 m is applied to all three axes.

The plots show the effect of the increase in weights on the variability of the solution. We do find a non-linear structure of the solution with the increase in weights. However, generally, higher order weights converge to a correct solution with the exception of the case where the translation is estimated (Figure 2(d)).

The optimal weights are empirically determined as $w_n = 10^5$ and $w_d = 10^5$ and used for the rest of the work.

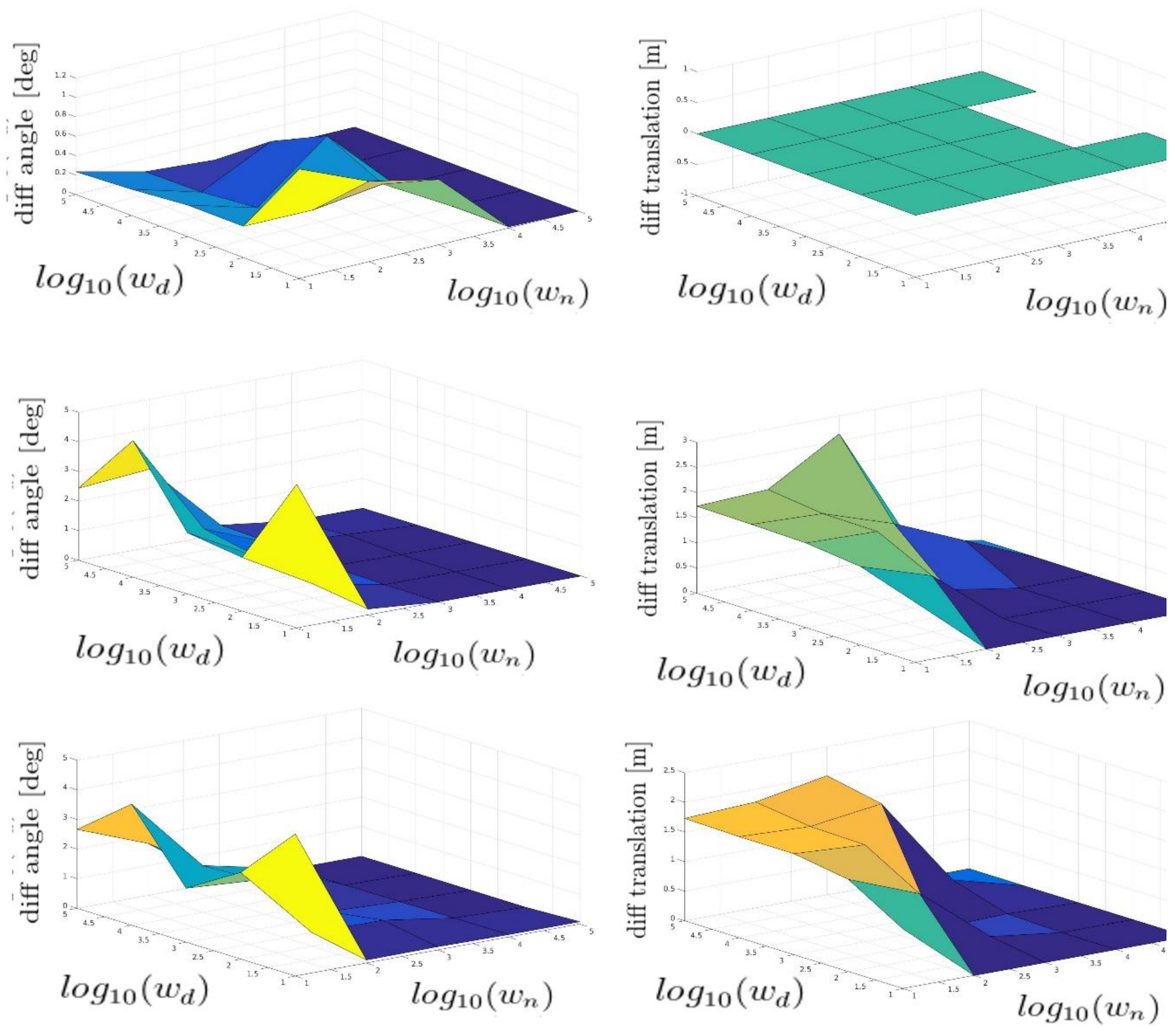

Figure 2. Difference in rotation and translation as a function of changing weights. Top row represents a simulated rotation of 1º in all axes; Center row represents a simulated translation of 1 m in all three axes; Bottom row represents a simulated rotation of 1º and a translation of 1 m in all three axes. Left side plots show the sum of difference in rotation angles. Right side plots show the sum of difference in translation parameters

Comparison with other registration methods

The accuracy and efficiency of the proposed method needs to be compared and contrasted with other related methods. Ten indoor laser scans from the Velodyne HDL-32E scanner mentioned above, is used for registration. The reference values are generated by manual alignment of artificial targets, with accuracy in the sub-millimeter range. The proposed registration algorithm is compared to the actual parameters and also to GICP (Segal et al, 2009). GICP is chosen due to it being a state-of-the-art approach in point-based registration method. The plane-based coarse registration method (Brenner et al, 2008) was also used in comparison but did not converge to transformation parameters close to the accurate solution and thus was not included in the results.

The results of the transformation parameters of the methods are presented in Tables 1 and 2. All the scan pairs are matched using GICP with default parameters. The actual transformation parameters are used to calculate the difference in the estimated transformation parameters using GICP and the proposed method. As can be seen in Table 1, GICP estimates the rotation parameters to be equal to the initial parameters while probabilistic matching technique gives results which are close to the actual solution. Similarly, with translation (Table 2), GICP overestimates the solutions in most of the cases while probabilistic matching technique gives translation parameters close to the actual results. In terms of speed, GICP takes close to 100 iterations to compute the transformation parameter values while probabilistic matching takes 2-3 iterations for each of the pairs. However, there is an additional cost for the plane segmentation in the latter case. This is minimized by using a parallel algorithm with voxels and region growing. Thus, even with the planar segmentation, the entire probabilistic matching algorithm comes under the time budget of GICP.

CONCLUSIONS

In this paper, a probabilistic paradigm of matching planes in two different datasets is defined. Using a probabilistic instead of a heuristic approach leads to a robust formulation of matching criteria with respect to occlusions and changing viewpoints while preserving the speed and accuracy similar to GICP. The registration is transformed into iterative EM algorithm which has its benefits with convergence happening in successive steps while weeding out the incorrect correspondences. The expectation step revolves around the formulation of the matching matrix using the principle of maximum entropy with a generic cost function. For planar surfaces, definition of a cost function is an additive effect of similarity of the planar normals and distances to the origin multiplied by weights. Weights are chosen a priori to be discriminative and are not modified.

In the maximization step, for a given matching matrix, the optimal transformation parameters are determined. Determination of rotation is straightforward with the matching matrix added as a weight to the previous binary-weighted definition. Translation determination is more complicated in case of uncertain correspondences since we cannot use the simple OLS criterion. An approximate LTS criterion is used as an convex optimization to remove incorrect correspondences and calculate the translation.

The coarse registration algorithm would be unbounded in errors without assistance of odometry or inertial system. Future work would be to use matching matrices from multiple scans to correct the coarse registration error. Utilizing a bundle adjustment sort of algorithm with the matching matrices as weights, the corrections to each of the different scans can be provided. The result should yield a consistent 3D model without the use of odometry or artificial markers.

Even though the proposed approach has been used for planar matching, another future work can extend this technique for any primitive shape such as cylinders. In that case, the matching matrix will be defined in the same fashion but the cost function will need a different distance criterion and finding the optimal transformation parameters would have to be changed similarly.

Table 1: Table shows comparison of the translation parameters between the various registration methods. The rotation is measured in **degree**

Frame pair	Actual parameters [°]	GICP parameters [1] [°]	Δ GICP [°]	Probabilistic parameters [°]	Δ probabilistic [°]
1-2	[-6.591,7.681,0.550]	[0.000,0.000,0.000]	[-6.591,7.681,0.550]	[-0.576,0.463,-0.165]	[-6.015,7.218,0.715]
2-3	[-3.229,3.831,0.321]	[0.000,0.000,0.000]	[-3.229,3.831,0.321]	[-4.179,0.697,4.127]	[0.95,3.134,-3.806]
3-4	[7.188,-6.651,-0.533]	[0.000,0.000,0.000]	[7.188,-6.651,-0.533]	[9.711,-0.419,-0.306]	[-2.523,-6.232,-0.227]
4-5	[-4.204,3.846,-0.492]	[0.000,0.000,0.000]	[-4.204,3.846,-0.492]	[-7.979,7.633,-0.919]	[3.775,-3.787,0.427]
5-6	[-5.225,4.911,0.307]	[0.000,0.000,0.000]	[-5.225,4.911,0.307]	[-10.532,4.168,6.899]	[5.307,0.742,-6.592]
6-7	[-5.665,5.636,0.561]	[0.000,0.000,0.000]	[-5.665,5.636,0.561]	[-0.323,7.712,5.764]	[-5.342,-2.076,-5.203]
7-8	[-4.172,4.867,1.653]	[0.000,0.000,0.000]	[-4.172,4.867,1.653]	[-3.944,1.899,8.800]	[-0.228,2.968,-7.147]
8-9	[-5.814,5.780,-0.416]	[0.000,0.000,0.000]	[-5.814,5.780,-0.416]	[-7.116,7.820,-0.969]	[1.302,-2.04,0.553]
9-10	[-3.944,4.824,-2.370]	[0.000,0.000,0.000]	[-3.944,4.824,-2.370]	[-6.948,5.074,0.237]	[3.004,-0.25,-2.607]

Table 2: Table shows comparison of the translation parameters between the various registration methods. The displacement is measured in **m**

Frame pair	Actual parameters [m]	GICP parameters [1] [m]	Δ GICP [m]	Probabilistic parameters [m]	Δ probabilistic [m]
1-2	[0.122,-0.101,0.136]	[0.200,0.001,-0.001]	[-0.078,-0.102,0.137]	[0.041,0.001,0.014]	[0.081,-0.102,0.122]
2-3	[0.019,-0.079,-0.095]	[0.114,0.001,0.001]	[-0.095,-0.08,-0.096]	[0.008,-0.113,0.018]	[0.011,0.034,-0.113]
3-4	[-0.133,0.177,0.151]	[0.383,0.001,-0.001]	[-0.516,0.176,0.152]	[-0.067,0.086,0.016]	[-0.066,0.091,0.135]
4-5	[0.065,-0.122,-0.137]	[0.170,0.001,0.001]	[-0.105,-0.123,-0.138]	[0.013,0.010,0.024]	[0.052,-0.132,-0.161]
5-6	[0.052,-0.105,-0.092]	[0.091,0.001,0.001]	[-0.039,-0.106,-0.093]	[0.014,0.012,-0.001]	[0.038,-0.117,-0.091]
6-7	[0.121,-0.078,-0.053]	[0.000,0.000,0.000]	[0.121,-0.078,-0.053]	[0.118,-0.007,-0.012]	[0.003,-0.071,-0.041]
7-8	[0.112,-0.063,-0.053]	[-0.001,0.001,0.000]	[0.113,-0.064,-0.053]	[-0.009,0.058,-0.003]	[0.121,-0.121,-0.05]
8-9	[0.140,-0.011,0.021]	[0.000,0.000,0.000]	[0.140,-0.011,0.021]	[0.121,0.011,-0.009]	[0.019,-0.022,0.03]
9-10	[0.143,0.016,-0.067]	[-0.141,0.000,0.000]	[-0.284,0.016,-0.067]	[0.075,0.032,-0.021]	[0.068,-0.016,-0.046]

REFERENCES

Segal, A., Haehnel, D. and Thrun, S., 2009, June. Generalized-icp. In *Robotics: science and systems* (Vol. 2, No. 4, p. 435).

Li, R., 1997. Mobile mapping: An emerging technology for spatial data acquisition. *Photogrammetric Engineering and Remote Sensing*, *63*(9), pp.1085-1092.

El-Hakim, S.F., Boulanger, P., Blais, F., Beraldin, J.A. and Roth, G., 1997. A mobile system for indoors 3-D mapping and positioning. *Proceedings of the Optical*, pp.275-282.

Besl, P.J. and McKay, N.D., 1992, April. Method for registration of 3-D shapes. In *Sensor Fusion IV: Control Paradigms and Data Structures* (Vol. 1611, pp. 586-607). International Society for Optics and Photonics.

Khoshelham, K., 2010, September. Automated localization of a laser scanner in indoor environments using planar objects. In *Indoor Positioning and Indoor Navigation (IPIN), 2010 International Conference on* (pp. 1-7). IEEE.

Douadi, L., Aldon, M.J. and Crosnier, A., 2006, October. Pair-wise registration of 3D/color data sets with ICP. In *Intelligent Robots and Systems, 2006 IEEE/RSJ International Conference on* (pp. 663-668). IEEE.

Schutz, C., Jost, T. and Hugli, H., 1998, August. Multi-feature matching algorithm for free-form 3D surface registration. In *Pattern Recognition, 1998. Proceedings. Fourteenth International Conference on* (Vol. 2, pp. 982-984). IEEE.

Rusinkiewicz, S. and Levoy, M., 2001. Efficient variants of the ICP algorithm. In *3-D Digital Imaging and Modeling, 2001. Proceedings. Third International Conference on* (pp. 145-152). IEEE.

Rangarajan, A., Chui, H., Mjolsness, E., Pappu, S., Davachi, L., Goldman-Rakic, P. and Duncan, J., 1997. A robust point-matching algorithm for autoradiograph alignment. *Medical image analysis*, *1*(4), pp.379-398.

Rangarajan, A., Chui, H. and Duncan, J.S., 1999. Rigid point feature registration using mutual information. *Medical Image Analysis*, *3*(4), pp.425-440.

Granger, S., Pennec, X. and Roche, A., 2001, October. Rigid point-surface registration using an EM variant of ICP for computer guided oral implantology. In *International Conference on Medical Image Computing and Computer-Assisted Intervention* (pp. 752-761). Springer, Berlin, Heidelberg.

Higuchi, K., Hebert, M. and Ikeuchi, K., 1995. Building 3-D models from unregistered range images. *Graphical models and image processing*, *57*(4), pp.315-333.

Chua, C.S. and Jarvis, R., 1996. 3D free-form surface registration and object recognition. *International journal of computer vision*, *17*(1), pp.77-99.

Rabbani, T., Dijkman, S., van den Heuvel, F. and Vosselman, G., 2007. An integrated approach for modelling and global registration of point clouds. *ISPRS journal of Photogrammetry and Remote Sensing*, *61*(6), pp.355-370.

Brenner, C., Dold, C. and Ripperda, N., 2008. Coarse orientation of terrestrial laser scans in urban environments. *ISPRS journal of photogrammetry and remote sensing*, *63*(1), pp.4-18.

He, W., Ma, W. and Zha, H., 2005, June. Automatic registration of range images based on correspondence of complete plane patches. In *3-D Digital Imaging and Modeling, 2005. 3DIM 2005. Fifth International Conference on* (pp. 470-475). IEEE.

Wang, M. and Tseng, Y.H., 2004. Lidar data segmentation and classification based on octree structure. *parameters*, *1*, p.5.

Bae, K.H. and Lichti, D., 2004. Edge and tree detection from three-dimensional unorganised point clouds from terretrial laser scanners. In *Proceedings of 12 Australasian Remote Sensing and Photogrammetry Conference* (pp. 1-9). Spatial Sciences Institute.

Gruen, A. and Akca, D., 2005. Least squares 3D surface and curve matching. *ISPRS Journal of Photogrammetry and Remote Sensing*, *59*(3), pp.151-174.

Dold, C. and Brenner, C., 2006. Registration of terrestrial laser scanning data using planar patches and image data. *International Archives of Photogrammetry, Remote Sensing and Spatial Information Sciences*, *36*(5), pp.78-83.

Pathak, K., Birk, A., Vaskevicius, N. and Poppinga, J., 2010. Fast registration based on noisy planes with unknown correspondences for 3-D mapping. *IEEE Transactions on Robotics*, *26*(3), pp.424-441.

Wang, M. and Tseng, Y.H., 2011. Incremental segmentation of lidar point clouds with an octree-structured voxel space. *The Photogrammetric Record*, *26*(133), pp.32-57.

Yang, X. and Meer, P., 2016. Robust Estimation of Multiple Inlier Structures. *arXiv preprint arXiv:1609.06371*.

Jaynes, E.T., 1957. Information theory and statistical mechanics. *Physical review*, *106*(4), p.620.

Horn, B.K., 1987. Closed-form solution of absolute orientation using unit quaternions. *JOSA A*, *4*(4), pp.629-642.

Shen, F., Shen, C., van den Hengel, A. and Tang, Z., 2013. Approximate least trimmed sum of squares fitting and applications in image analysis. *IEEE Transactions on Image Processing*, *22*(5), pp.1836-1847.